

First-Principles Prediction of Rate Coefficients for Free-Radical Cyclization Reactions at Selenium

Sofia Lobachevsky,^{†,‡} Carl H. Schiesser,^{†,‡} Ching Yeh Lin,^{†,§} and Michelle L. Coote^{*,†,§}

ARC Centre of Excellence for Free Radical Chemistry and Biotechnology and School of Chemistry, Bio21 Molecular Science and Biotechnology Institute, University of Melbourne, Victoria, 3010 Australia, and Research School of Chemistry, Australian National University, Canberra ACT 0200, Australia

Received: July 24, 2008; Revised Manuscript Received: October 21, 2008

High-level ab initio calculations of the barriers, enthalpies, and rate coefficients for the intramolecular cyclization reactions of $\bullet\text{CH}_2\text{CH}_2\text{CH}_2\text{CH}_2\text{SeR}$ ($\text{R} = \text{Me}, n\text{-Bu}, s\text{-Bu}, t\text{-Bu}, \text{Bn}, \text{Bz}, \text{Ph}_2\text{CH}$) and $\bullet\text{CH}_2\text{CH}_2\text{CH}_2\text{CH}_2\text{CH}=\text{CH}_2$ have been performed at the G3(MP2)-RAD level. The calculated rate coefficients show excellent agreement with experiment (to within a factor of 5 or better), although this might be due, in part, to a systematic cancellation of order-of-magnitude errors in the corresponding Arrhenius parameters. The intramolecular cyclizations at selenium were found to be energetically favorable processes that occur with synthetically accessible rate coefficients on the order of $10^4\text{--}10^6\text{ s}^{-1}$ at 294 K. These values are largely governed by the stabilization energy of the leaving radical, though with contributions from steric and polar effects.

Introduction

In the rapidly developing field of free-radical chemistry, the process of homolytic substitution plays a significant role. In particular, it has been recognized as a convenient method for carbon–heteroatom bond formation both inter- and intramolecularly.¹ Among other synthetic applications, intramolecular homolytic substitution has been successfully used in the construction of O-, S- and Se-containing heterocycles.² Se-containing heterocycles are of particular interest, as they exhibit a wide array of biological properties, including anticancer, antibacterial, antiviral, and antioxidant activities.³

Given that the successful design of radical reactions relies on the knowledge of the rates of the individual steps, a thorough understanding and development of intramolecular homolytic substitution at selenium as a synthetic tool depends on the availability of the relevant kinetic data. Unfortunately, obtaining kinetic data for ring closures can frequently be a synthetically and/or experimentally challenging task, and as a result, experimental kinetic data for intramolecular homolytic substitution at Se are somewhat limited. To date, only rate constants for attack by an aryl radical to displace the benzyl radical ($3 \times 10^7\text{ s}^{-1}$ at 80 °C)⁴ and attack by a primary alkyl radical to displace a diphenylmethyl radical ($1 \times 10^7\text{ s}^{-1}$ at 25 °C)⁵ have been reported, with both studies indicating the formation of tetrahydro-selenophene. Because studies of bimolecular homolytic substitution at Se suggest pronounced leaving radical effects,⁶ it is of interest to examine the cyclization kinetics for a much wider range of leaving groups.

Computational chemistry offers a complementary method for studying reaction kinetics and can be particularly useful for free-radical processes, where the possibility of competing side reactions can sometimes hamper experimental measurements. To date, there do not appear to have been any high-level

computational studies of the kinetics of intramolecular homolytic substitution at Se or of the effects of the leaving group. However, earlier studies examined the mechanism of this reaction in simple ω -chalcogenylalkyl radicals.^{7,8} Mechanistically, homolytic substitution is much like nonradical nucleophilic substitution, except that solvation is of much less importance in neutral radical environments. Evidence exists for two possible mechanisms: one is a concerted process, whereby radical R^\bullet forms a bond to atom Y simultaneously with homolytic scission of the Y–L bond, resulting in the formation of radical L^\bullet ; the other involves formation of a transient hypervalent intermediate $[\text{R}\cdots\text{Y}\cdots\text{L}]^\bullet$.^{1,7}



Both intermolecular and intramolecular homolytic substitution at O, S, and Se are predicted to proceed via a concerted mechanism with a transition state having a collinear or nearly so arrangement of attacking and leaving radicals.^{9,10} On the other hand, Te group transfer appears to involve a transient hypervalent intermediate, which is presumably due to the increased availability of its low-lying d orbitals.⁷ A concerted mechanism for homolytic substitution at Se is consistent with the experimental evidence for large leaving-group effects on the intermolecular reaction kinetics⁶ and suggests that similar effects would be expected for the analogous intramolecular reaction.

In the present work, we use high-level ab initio molecular orbital calculations to study intramolecular homolytic substitution at Se for the series of radicals $\bullet\text{CH}_2\text{CH}_2\text{CH}_2\text{CH}_2\text{SeR}$ for $\text{R} = \text{Me}, n\text{-Bu}, s\text{-Bu}, t\text{-Bu}, \text{Bz}, \text{Bn},$ and Ph_2CH , with a view toward studying the effect of the leaving group R (see Scheme 1). We also examine the ability of high-level ab initio molecular orbital calculations to reproduce the available experimental data for these and related reactions, with a view toward establishing a reliable theoretical methodology that can be applied in cases where experimental data are not available.

Computational Procedures

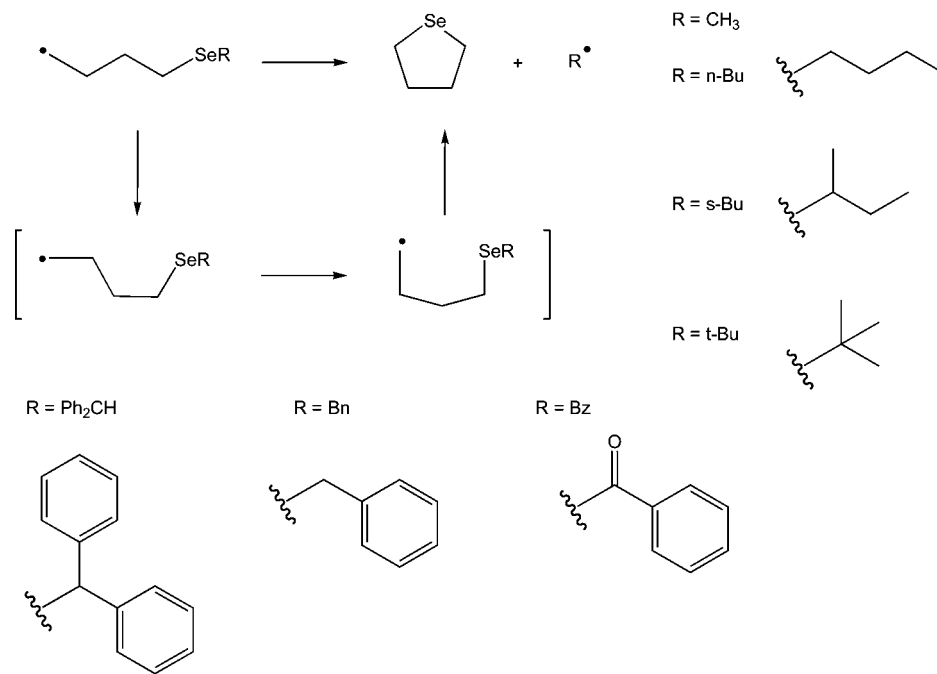
Standard ab initio molecular orbital theory and density functional theory calculations were carried out using Gaussian

* Author for correspondence. E-mail: mcoote@rsc.anu.edu.au.

[†] ARC Centre of Excellence for Free Radical Chemistry and Biotechnology, University of Melbourne.

[‡] Bio21 Molecular Science and Biotechnology Institute, University of Melbourne.

[§] Australian National University.

SCHEME 1: Cyclization of $\bullet\text{CH}_2\text{CH}_2\text{CH}_2\text{CH}_2\text{SeR}$ 

03¹¹ and MOLPRO 2000.6¹² software. Geometries and frequencies were obtained at the B3-LYP/6-31G(d) level of theory, and extensive conformational searches were also performed at this level. All frequencies were scaled by their appropriate scale factors.¹³ We have previously shown that low levels of theory such as B3-LYP/6-31G(d) provide sufficiently accurate geometries and (scaled) frequencies for other radical reactions, including addition to various types of double bonds and hydrogen-atom abstraction.¹⁴ Improved energies were then obtained using G3(MP2)-RAD, a high-level composite method that approximates (U)RCCSD(T) calculations with a large triple- ζ basis set via additivity corrections at the R(O)MP2 level of theory.¹⁵ This approach has been shown to reproduce a large test set of gas-phase experimental data to within chemical accuracy,¹⁵ and we have had similar success with the use of this method to model the kinetics and thermodynamics of radical reactions such as addition and β -scission.¹⁶ Further evaluations of the accuracy of the present calculations are carried out below.

For the cyclizations of $\bullet\text{CH}_2\text{CH}_2\text{CH}_2\text{CH}_2\text{SeR}$ with $\text{R} = \text{Bz}$, Bn , and Ph_2CH , the reactant radicals were too large for practical G3(MP2)-RAD calculations to be performed using our computing resources. In those cases, we instead adopted an ONIOM approximation in which G3(MP2)-RAD calculations were performed for the “core” reaction (in this case, the corresponding reaction but with $\text{R} = \text{Me}$). These were then corrected for the substituent of the real R group, as calculated at the R(O)MP2/6-311+G(3df,2p) level of theory. We have recently shown that this approach yields an excellent approximation to full G3(MP2)-RAD calculations for a wide range of radical reactions.¹⁷ In the present work, we further test the ONIOM approximation through comparison with full G3(MP2)-RAD calculations for the case of $\text{R} = t\text{-Bu}$.

After the geometries, frequencies, and improved energies had been obtained, partition functions and corresponding thermodynamic functions (i.e., enthalpy H , entropy S , and Gibbs free energy G) were calculated using the standard textbook formulas, based on the statistical thermodynamics of an ideal gas under the harmonic-oscillator/rigid-rotor approximation.¹⁸ Further details of these formulas are provided in the Supporting

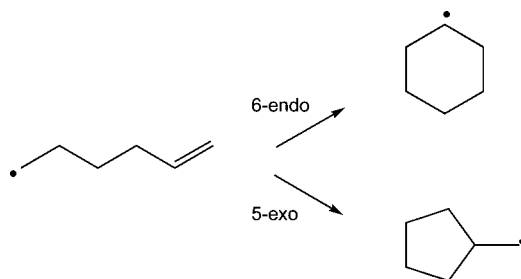
Information. For the overall cyclization reactions, we further corrected the rate coefficients by treating all low-frequency torsional modes as hindered internal rotations using the standard one-dimensional torsional eigenvalue summation (TES) method,¹⁹ applied at a 60° resolution. Our recent assessment study of 644 rotations in 104 organic molecules showed that this resolution is sufficient to reproduce the results obtained at the more accurate 10° resolution to within a factor of 1.08.²⁰ To mitigate the effects of coupling between the modes, we use the method of Van Cauter et al.²¹ for combining the hindered-rotor partition for the specific mode with the harmonic-oscillator partition functions for the remaining vibrational modes. In this method, the harmonic-oscillator approximation to all $3N - 6$ internal modes of a molecule, and the resulting vibrational partition function, is then multiplied by a correction factor for each internal hindered-rotor partition function. This factor is then calculated as the ratio of the hindered-rotor partition function to the corresponding “pure” vibrational partition function, as calculated from second derivative of the rotational potential.

In the present work, we calculate only the gas-phase rate coefficients and do not include corrections for solvent effects, as such effects are difficult to model accurately for transition structures. Moreover, based on a comparison of experimental gas- and solution-phase rate coefficients for other unimolecular cyclization reactions (such as the 5-hexenyl radical, which is studied in more detail below), we do not expect them to be significant for the present reactions.

Finally, to assist in the qualitative rationalization of the results, radical stabilization energies (RSEs) of the leaving radicals, $\text{R}\bullet$, were calculated at the G3(MP2)-RAD level of theory. These were defined in the usual manner²² as the enthalpies of reaction 2



for the various radicals, $\text{R}\bullet$. The charge distributions in the transition states and reactant radicals were also calculated on the basis of a natural bond orbital (NBO) population analysis,

SCHEME 2: Cyclization of $\bullet\text{CH}_2\text{CH}_2\text{CH}_2\text{CH}_2\text{CH}=\text{CH}_2$ 

carried out in Gaussian using the B3LYP/6-311+G(3df,2p) density.

Results

Kinetic and thermodynamic parameters were calculated for the cyclization reactions of $\bullet\text{CH}_2\text{CH}_2\text{CH}_2\text{CH}_2\text{SeR}$ (for $\text{R} = \text{Me}$, $n\text{-Bu}$, $s\text{-Bu}$, $t\text{-Bu}$, Bz , Bn , and Ph_2CH) and $\bullet\text{CH}_2(\text{CH}_2)_3\text{CH}=\text{CH}_2$. These reactions are depicted in Schemes 1 and 2, respectively. The 6-endo cyclization of the latter radical was chosen for benchmarking of the theoretical calculations, as both gas-phase²³ and solution-phase²⁴ experimental data are available for it. We also considered the more common 5-exo reaction, although, in this case, we could locate only solution-phase²⁴ experimental data. In all cases, cyclization proceeds via a series of steps in which the global minimum-energy conformation of the radical undergoes rotation to form a “curled” intermediate, from which cyclization can then proceed. Figure 1 shows the free energy diagram corresponding to these individual steps for the $\bullet\text{CH}_2\text{CH}_2\text{CH}_2\text{CH}_2\text{SeR}$ radicals for $\text{R} = \text{Me}$, Bu , $s\text{-Bu}$, and $t\text{-Bu}$, together with the corresponding optimized geometries for the $\text{R} = \text{Me}$ case. Optimized geometries of the cyclization transition structures for all of the $\bullet\text{CH}_2\text{CH}_2\text{CH}_2\text{CH}_2\text{SeR}$ radicals are shown in Figure 2; optimized geometries of all species are provided in the Supporting Information.

From Figure 1, it can be seen that, for each studied R group, the cyclization step has a much higher reaction barrier than the conformational changes that precede it and, hence, is rate-determining. As a result, the overall cyclization rate (i.e., as would be observed experimentally) is simply given by the product of the equilibrium constant(s) for the curling reaction(s) and the rate coefficient of the cyclization step itself. This, in turn, is equivalent to calculating the rate coefficient for the cyclization reaction from the global minimum-energy conformation of the reactant, rather than the curled intermediate. Therefore, to simplify the calculations, for the larger R groups

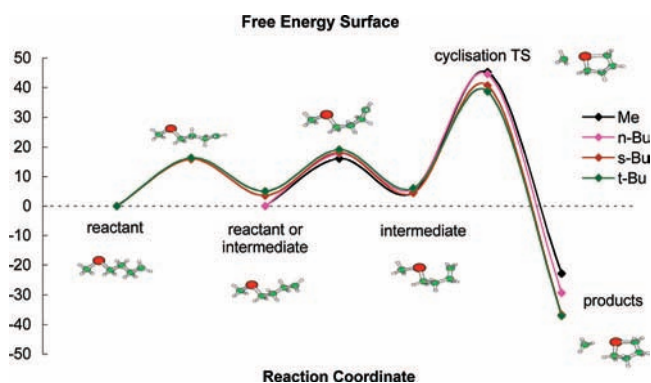


Figure 1. Free energy surface for cyclization of $\bullet\text{CH}_2\text{CH}_2\text{CH}_2\text{CH}_2\text{SeR}$ ($\text{R} = \text{Me}$, Bu , $s\text{-Bu}$, $t\text{-Bu}$).

($\text{R} = \text{Bz}$, Bn , and Ph_2CH) and for $\bullet\text{CH}_2(\text{CH}_2)_3\text{CH}=\text{CH}_2$, we simply calculated the overall cyclization rate in this manner.

Table 1 reports the enthalpies, entropies, and free energies of activation and reaction associated with the cyclization reactions of $\bullet\text{CH}_2\text{CH}_2\text{CH}_2\text{CH}_2\text{SeR}$. For the smaller R groups ($\text{R} = \text{Me}$, Bu , $s\text{-Bu}$, and $t\text{-Bu}$), thermodynamic data are included for all of the individual steps, together with those for the overall reaction; for the larger R groups ($\text{R} = \text{Bz}$, Bn , and Ph_2CH), only data for the overall reactions are included. Corresponding rate coefficients and Arrhenius parameters for the overall cyclization reactions of all radicals, together with the available experimental data from the literature, are listed in Table 2. For $\text{R} = t\text{-Bu}$, two sets of data are shown in Table 1; one is based on full G3(MP2)-RAD calculations, and the other uses an ONIOM approximation in which G3(MP2)-RAD calculations for the $\text{R} = \text{Me}$ system are combined with R(O)MP2/6-311+G(3df,2p) calculations of the R -group substituent effect. The latter are provided so as to enable testing of the ONIOM approximation, which is used for the larger R groups ($\text{R} = \text{Bz}$, Bn , and Ph_2CH).

Discussion

Assessment. If we first examine the rate coefficients and Arrhenius parameters for the 6-endo cyclization of the hexenyl radical (Table 2), we note that the gas- and solution-phase experimental data show close agreement with one another, indicating that, as expected, solvent effects are not significant in this reaction and are thus not likely to be significant in the other studied cyclizations. The calculated rate coefficient for this reaction shows excellent agreement with both the gas- and solution-phase values; however, the Arrhenius parameters exhibit slightly larger discrepancies. In essence, the theoretical calculations overestimate the frequency factor by approximately 1 order of magnitude, although this is then compensated by an equivalent overestimate of the reaction barrier. The gas-phase calculations for the more common 5-exo cyclization reaction also show good agreement with the solution-phase experimental data, although the frequency factor and barriers are again overestimated slightly by theory. Similar trends are also observed for the cyclizations at selenium: Where comparison is possible, theory reproduces the experimental rate coefficients to within a factor of 5 or better but overestimates the frequency factors by approximately an order of magnitude, with compensating errors in the activation energies.

Because of the scarcity of experimental data for these systems, it is difficult to account unambiguously for the discrepancies in the Arrhenius parameters. On one hand, because the theoretical calculations were calculated for gas-phase reactions and the majority of the experimental data were measured in solution, it is possible that the results reflect fundamental gas-phase versus solution-phase differences in cyclization kinetics. It is true that the gas- and solution-phase experimental data for the 6-endo hexenyl radical cyclization show close agreement with one another; however, it should be noted that the Arrhenius parameters in the gas-phase study of this reaction were assumed, rather than measured. On the other hand, the discrepancies might reflect genuine error in the calculations and/or experiments. It is worth noting that, for other types of radical reactions such as additions to alkenes, it has been shown that it is difficult to obtain accurate and precise experimental measurements of the Arrhenius parameters, even when rate coefficients can be measured with a high degree of accuracy. Rather, owing to the relatively narrow temperature ranges typically involved, the 95% joint confidence intervals for Arrhenius parameters tend to be

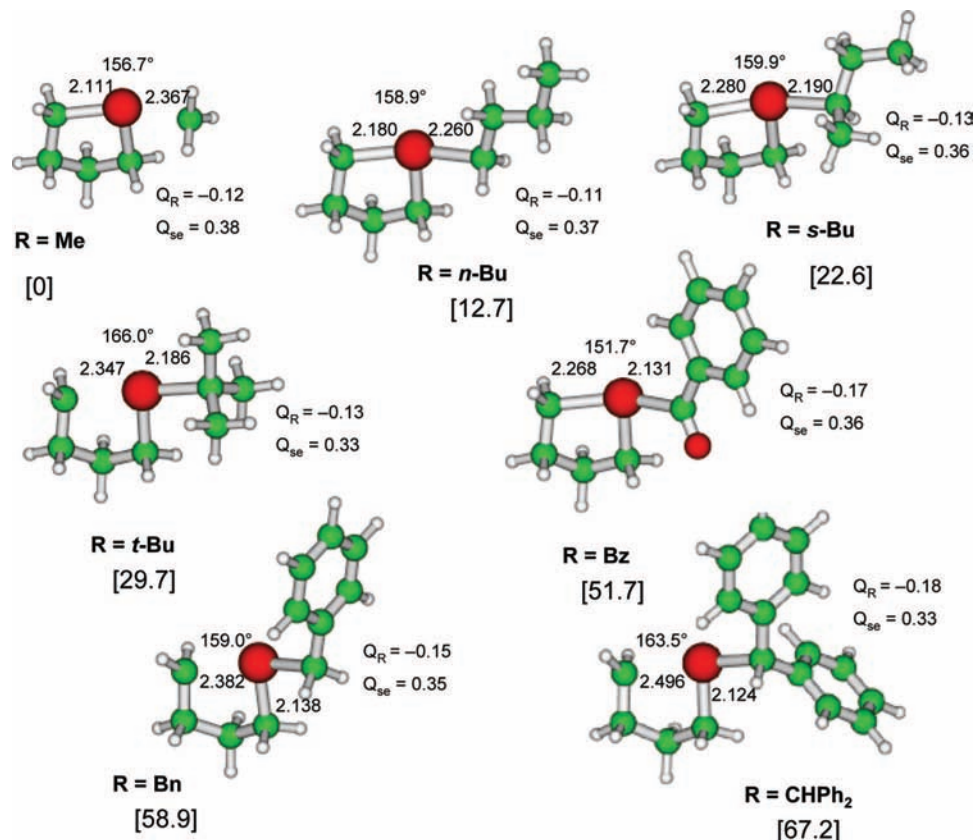


Figure 2. B3-LYP/6-31G(d)-optimized geometries of the transition structures for the cyclization of $\bullet\text{CH}_2\text{CH}_2\text{CH}_2\text{CH}_2\text{SeR}$ showing the natural charges on R (Q_R) and Se (Q_{se}), the lengths (Å) of the forming and breaking bonds, and the angle they make with one another. The numbers in square brackets are the radical stabilization energies (kJ mol⁻¹) of R \bullet .

large and highly correlated with one another.²⁵ Indeed, for radical additions to alkenes, it has even been suggested that, given this problem, theoretical calculations should be used to obtain the frequency factors of reactions, which can then be combined with experimental rate coefficients so as to obtain experimental activation energies.^{25b} In any case, it would be desirable to probe this discrepancy through further experimental studies of these reactions, and these are currently underway in our laboratories.

Finally, for the case of the $\bullet\text{CH}_2\text{CH}_2\text{CH}_2\text{CH}_2\text{SeC}(\text{CH}_3)_3$ radical, it is possible to compare the results obtained with and without the use of the ONIOM approximation (see Table 1). In general, the differences in the enthalpies of activation and reaction for each of the reaction steps in the cyclization process are negligible (less than 1 kJ mol⁻¹). The only exception to this is the enthalpy of the cyclization reaction, for which the difference is somewhat larger (6.5 kJ mol⁻¹), though still close to the average error expected at the G3(MP2)-RAD level of theory itself (ca. 5.2 kJ mol⁻¹).²⁵ This exceptional case corresponds to the only calculation in which the Se—R bond is fully broken; in the curling reactions and the cyclization barrier, the species involved remain structurally similar and benefit from systematic cancellation of error. It would appear that full G3(MP2)-RAD calculations (or at least inclusion of additional substituents on R in the reaction core of the ONIOM calculation) might be necessary for the accurate calculation of the Se—R bond energy; however, the ONIOM approximation is suitable for calculations of the cyclization kinetics.

Mechanistic Aspects. The intramolecular cyclization of $\bullet\text{CH}_2\text{CH}_2\text{CH}_2\text{CH}_2\text{SeR}$ (R = Me, *n*-Bu, *s*-Bu, *t*-Bu, Bn, Bz, Ph₂CH) is an energetically favorable process and occurs with synthetically accessible rate coefficients on the order of 10⁴–10⁶

s⁻¹. As in the case of bimolecular homolytic substitution,^{6a} the intramolecular rate coefficients are substantially higher than those for analogous reactions at sulfur (e.g., 14.33 s⁻¹ at 21 °C for R = *n*-Pr, 7.0 × 10³ s⁻¹ at 50 °C for R = Bz),²⁶ which is presumably due to the considerably weaker R—Se versus R—S bonds.

As expected, the ring closures at Se are concerted and proceed via transition states with nearly collinear geometries, having angles between attacking and leaving radicals ranging from 151.7° to 166.0° (Figure 2). The key features of the transition-state geometries are relatively unaffected by the nature of the R group, although those for reactions having lower barriers and greater exothermicities (such as the R = Bn and Ph₂CH reactions) tend to be earlier in accordance with the Hammond postulate. Not surprisingly, the frequency factors for the reactions are also calculated to be very similar to one another, with only R = Bz and Bn having higher values than the others, possibly reflecting the greater gain in flexibility in the transition state as orbital interactions between the selenium and π systems are disrupted in these radicals.

The barrier heights for the overall cyclization reactions tend to follow expectations on the basis of the radical stabilization energy (RSE) of the leaving radical; thus, radicals with stabilized leaving groups such as Ph₂CH and Bn have lower barriers than those with less stabilized radicals such as Me and *n*-Bu (see Figure 3). However, the correlation is not perfect; in particular, Bn and Bz have slightly higher barriers than might have been predicted on the basis of stability alone. This might reflect reduced steric crowding in their reactant radicals, when compared with species having secondary and tertiary substituted R groups, or the stronger orbital interactions between Se and the

TABLE 1: Enthalpies (H , kJ mol⁻¹), Entropies (S , J mol⁻¹ K⁻¹), and Free Energies (G , kJ mol⁻¹) for the Cyclization of •CH₂CH₂CH₂CH₂SeR at 21 °C^a

R	ΔH (kJ/mol)	ΔS (J/Kmol)	ΔG (kJ/mol)	ΔH^\ddagger (kJ/mol)	ΔS^\ddagger (J/Kmol)	ΔG^\ddagger (kJ/mol)
Step 1						
Me	1.8	-10.0	4.7	9.9	-22.5	16.5
<i>n</i> -Bu	1.4	-14.9	5.8	9.7	-27.4	17.7
<i>s</i> -Bu	1.5	-7.3	3.6	9.9	-20.2	15.9
<i>t</i> -Bu	1.3	-12.5	5.0	10.0	-21.4	16.3
<i>t</i> -Bu ^b	1.1	-12.5	4.8	10.0	-21.4	16.3
Step 2						
Me	—	—	—	—	—	—
<i>n</i> -Bu	—	—	—	—	—	—
<i>s</i> -Bu	-0.1	-3.1	0.8	8.6	-20.4	14.6
<i>t</i> -Bu	0.8	-0.6	1.0	8.7	-18.3	14.1
<i>t</i> -Bu ^b	1.2	-0.6	1.4	8.9	-18.3	14.2
Step 3						
Me	1.3	104.8	-29.5	32.8	-29.0	41.3
<i>n</i> -Bu	2.9	129.3	-35.2	29.4	-32.0	38.8
<i>s</i> -Bu	0.4	141.3	-41.1	26.7	-32.4	36.3
<i>t</i> -Bu	-0.6	152.5	-45.4	23.7	-30.7	32.8
<i>t</i> -Bu ^b	5.9	152.5	-38.9	24.6	-30.7	33.6
Overall						
Me	3.1	94.8	-24.7	34.6	-39.0	46.0
<i>n</i> -Bu	4.3	114.5	-29.3	30.8	-46.9	44.6
<i>s</i> -Bu	1.7	130.9	-36.7	28.1	-42.8	40.7
<i>t</i> -Bu	1.5	139.3	-39.4	25.8	-43.9	38.7
<i>t</i> -Bu ^b	8.2	139.3	-32.7	26.9	-43.9	39.8
Bz ^b	16.8	126.3	-20.3	28.6	-25.5	36.1
Bn ^b	-24.5	107.0	-56.0	23.7	-30.5	32.6
Ph ₂ CH ^b	-38.0	114.9	-71.8	14.3	-45.2	27.6

^a Calculated at the G3(MP2)-RAD level in conjunction with the harmonic-oscillator approximation. For R = Bz, B, and Ph₂CH, an ONIOM approximation was used; for R = *t*-Bu, the full G3(MP2)-RAD calculations and the corresponding ONIOM approximations are both included to provide a test of the latter. For R = Me, Bu, *s*-Bu, and *t*-Bu, thermochemical data are shown for each of the individual steps in the reaction, "curling" (steps 1 and, where relevant, 2) and cyclization of the curled radical (step 3), in addition to those for the overall reaction. For R = Bz, Bn, and Ph₂CH, only the overall thermochemical data are shown. ^b ONIOM results.

π systems of these R groups that are disrupted upon formation of the transition state.

Although the barrier heights show a reasonable correlation with the stability of the leaving radical ($R^2 = 0.715$), for the overall reaction enthalpies, the correlation with the RSEs is very poor ($R^2 = 0.380$). In particular, the R = Bz reaction is the most endothermic of the cyclizations despite giving rise to one of the more stabilized leaving radicals. This probably reflects the conjugation between the Se and the carbonyl in the reactant radical, which strengthens the breaking bond. With this species omitted, the correlation between RSE and enthalpy improves dramatically ($R^2 = 0.866$) but is still not perfect, as steric and polar effects contribute to the structure-reactivity trends. In particular, the Se—R bond is stabilized by resonance with Se⁺R⁻ configurations, as is evident in the calculated charges on R and Se that are on the order of -0.15 and +0.28, respectively (see Table S4 of the Supporting Information). This stabilizing effect, which varies with the R group, is of course absent in the neutral products and thus has a much greater influence on the reaction enthalpies than the barriers, where it cancels to some extent.

Conclusion

The intramolecular cyclization of •CH₂CH₂CH₂CH₂SeR (R = Me, *n*-Bu, *s*-Bu, *t*-Bu, Bn, Bz, Ph₂CH) is an energetically

TABLE 2: Theoretical and Experimental Values of the Rate Coefficient (k_c , s⁻¹) and Arrhenius Activation Energy (E_a , kJ mol⁻¹) and Frequency Factor (A , s⁻¹) for the Cyclization Reactions of •CH₂CH₂CH₂CH₂SeR and •CH₂CH₂CH₂CH₂CH=CH₂ at 21 °C^a

	theoretical ^a			experimental		
	k_c (s ⁻¹)	E_a (kJ/mol)	log A	k_c (s ⁻¹)	E_a (kJ/mol)	log A
•CH ₂ CH ₂ CH ₂ CH ₂ SeR						
R = Me	3.4×10^4	34.7	10.7	—	—	—
R = <i>n</i> -Bu	1.4×10^5	31.0	10.6	5.0×10^4 ^{c,d}	27.97	9.48
R = <i>s</i> -Bu	2.6×10^5	30.2	10.8	2.7×10^5 ^{c,d}	21.97	9.21
R = <i>t</i> -Bu	8.1×10^5	28.3	10.9	—	—	—
R = Bz ^b	2.7×10^6	31.2	12.0	1.6×10^6 ^d	15.80 ^e	9.00 ^e
R = Bn ^b	1.6×10^7	26.1	11.8	—	—	—
R = Ph ₂ CH ^b	3.6×10^7	17.5	10.7	9.5×10^6 ^f	10.60	8.86
•CH ₂ CH ₂ CH ₂ CH ₂ CH=CH ₂ (6-endo cyclization)						
gas phase	2.1×10^3	41.2	10.6	6.0×10^3 ^g	35.0	10.0 ^e
solution phase	—	—	—	3.4×10^3 ^h	35.6	9.85
•CH ₂ CH ₂ CH ₂ CH ₂ CH=CH ₂ (5-exo cyclization)						
gas phase	7.6×10^4	33.7	10.9	—	—	—
solution phase	—	—	—	2.0×10^5 ^h	28.5	10.35

^a Data correspond to the overall reaction. Theoretical values calculated at the G3(MP2)-RAD level in conjunction with the hindered-rotor model. For R = Bz, Bn, and Ph₂CH, an ONIOM approximation was used. ^b ONIOM results. ^c Experimental data for *n*-octyl and *sec*-octyl are used for *n*-butyl and *sec*-octyl, respectively. ^d Unpublished data. ^e log A value was estimated, and E_a was then calculated from the known rate constant and the estimated log A value. ^f Reference 5. ^g Reference 23. ^h Reference 24.

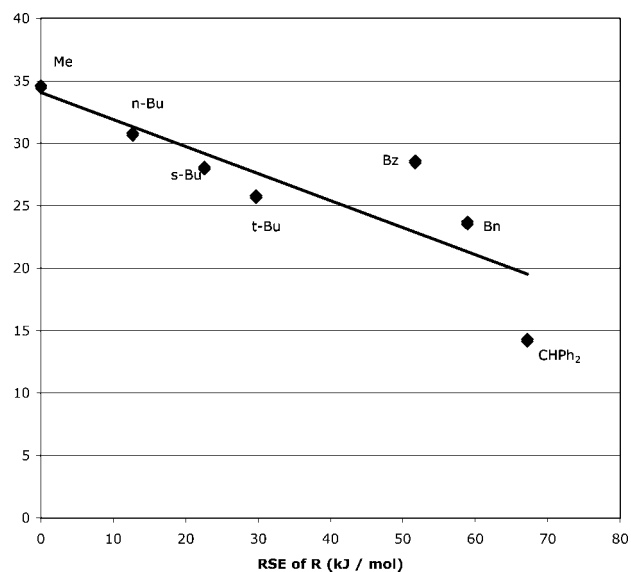


Figure 3. Relationship between the barrier height and radical stabilization energy (RSE) of the leaving group R in the cyclization of •CH₂CH₂CH₂CH₂SeR. The line of best fit has an R^2 value of 0.715.

favorable process and occurs with synthetically accessible rate coefficients on the order of 10^4 – 10^6 s⁻¹. The rate coefficients are largely governed by the stabilization energy of the leaving radical, though with contributions from steric and polar effects. Nonetheless, even for the poorest leaving groups, it is clear that the reactions hold synthetic potential for preparation of Se-containing heterocycles. Overall, it appears that the ab initio methodology used in the present work can provide chemically accurate values of the cyclization rate coefficients of these reactions at the studied temperature, although there remains the possibility of slightly larger errors in the Arrhenius parameters, which requires further investigation.

Acknowledgment. We gratefully acknowledge support from the Australian Research Council under their Centres of Excellence program and generous allocations of computing time on the National Facility of the Australian Partnership for Advanced Computing.

Supporting Information Available: Formulas used for the calculation of rate and equilibrium constants, B3LYP/6-31G(d)-optimized geometries of all species in the form of Gaussian archive entries, corresponding total energies and charge distributions in the reactant radicals. This material is available free of charge via the Internet at <http://pubs.acs.org>.

References and Notes

- Walton, J. C. *Acc. Chem. Res.* **1998**, *31*, 99–107.
- See, for example: (a) Montaudon, E.; Lubeigt, X.; Maillard, B. *J. Chem. Soc., Perkin Trans. 1* **1991**, *153*, 1–1538. (b) Coulomb, J.; Certal, V.; Fensterbank, L.; Lacote, E.; Malacria, M. *Angew. Chem., Int. Ed.* **2006**, *45*, 633–637. (c) Malmstroem, J.; Jonsson, M.; Cotgreave, I. A.; Hammarstroem, L.; Sjoedin, M.; Engman, L. *J. Am. Chem. Soc.* **2001**, *123*, 3434–3440. (d) Schiesser, C. H.; Zheng, S.-L. *Tetrahedron Lett.* **1999**, *40*, 5095–5098. (e) Fenner, T.; White, J. M.; Schiesser, C. H. *Org. Biomol. Chem.* **2006**, *4*, 466–474. (f) Carland, M. W.; Schiesser, C. H. *Molecules* **2004**, *9*, 466–471.
- See, for example: (a) May, S. W. *Expert Opin. Invest. Drugs* **1999**, *8*, 1017–1030. (aa) May, S. W. *Expert Opin. Invest. Drugs* **2002**, *11*, 1261–1269. (b) Mughesh, G.; du Mont, W.-W.; Sies, H. *Chem. Rev.* **2001**, *101*, 2125–2179.
- Lyons, J. E.; Schiesser, C. H.; Sutej, K. *J. Org. Chem.* **1993**, *58*, 5632–5638.
- Wild, L. M. Ph.D. Thesis, University of Melbourne, Victoria, Australia, 1998.
- (a) Scaiano, J. C.; Schmid, P.; Ingold, K. U. *J. Organomet. Chem.* **1976**, *121*, C4–C6. (b) Curran, D. P.; Martin-Esker, A. A.; Ko, S. B.; Newcomb, M. *J. Org. Chem.* **1993**, *58*, 4691–4695.
- Wild, L. M.; Schiesser, C. H. *Tetrahedron* **1996**, *52*, 13265–13314.
- Schiesser, C. H.; Wild, L. M. *J. Org. Chem.* **1999**, *64*, 1131–1139.
- Schiesser, C. H.; Smart, B. A. *Tetrahedron* **1995**, *51*, 6051–6060.
- Wijaya, C. D.; Sumathi, R.; Green, W. H., Jr. *J. Phys. Chem. A* **2003**, *107*, 4908–4920.
- Frisch, M. J.; Trucks, G. W.; Schlegel, H. B.; Scuseria, G. E.; Robb, M. A.; Cheeseman, J. R.; Montgomery, J. A., Jr.; Vreven, T.; Kudin, K. N.; Burant, J. C.; Millam, J. M.; Iyengar, S. S.; Tomasi, J.; Barone, V.; Mennucci, B.; Cossi, M.; Scalmani, G.; Rega, N.; Petersson, G. A.; Nakatsuji, H.; Hada, M.; Ehara, M.; Toyota, K.; Fukuda, R.; Hasegawa, J.; Ishida, M.; Nakajima, T.; Honda, Y.; Kitao, O.; Nakai, H.; Klene, M.; Li, X.; Knox, J. E.; Hratchian, H. P.; Cross, J. B.; Adamo, C.; Jaramillo, J.; Gomperts, R.; Stratmann, R. E.; Yazyev, O.; Austin, A. J.; Cammi, R.; Pomelli, C.; Ochterski, J. W.; Ayala, P. Y.; Morokuma, K.; Voth, G. A.; Salvador, P.; Dannenberg, J. J.; Zakrzewski, V. G.; Dapprich, S.; Daniels, A. D.; Strain, M. C.; Farkas, O.; Malick, D. K.; Rabuck, A. D.; Raghavachari, K.; Foresman, J. B.; Ortiz, J. V.; Cui, Q.; Baboul, A. G.; Clifford, S.; Cioslowski, J.; Stefanov, B. B.; Liu, G.; Liashenko, A.; Piskorz, P.; Komaromi, I.; Martin, R. L.; Fox, D. J.; Keith, T.; Al-Laham, M. A.; Peng, C. Y.; Nanayakkara, A.; Challacombe, M.; Gill, P. M. W.; Johnson, B.; Chen, W.; Wong, M. W.; Gonzalez, C.; Pople, J. A. *Gaussian 03*, revision B.03; Gaussian, Inc.: Pittsburgh, PA, 2003.
- Werner, H.-J.; Knowles, P. J.; Amos, R. D.; Bernhardsson, A.; Berning, A.; Celani, P.; Cooper, D. L.; Deegan, M. J. O.; Dobbyn, A. J.; Eckert, F.; Hampel, C.; Hetzer, G.; Korona, T.; Lindh, R.; Lloyd, A. W.; McNicholas, S. J.; Manby, F. R.; Meyer, W.; Mura, M. E.; Nicklass, A.; Palmieri, P.; Pitzer, R.; Rauhut, G.; Schütz, M.; Stoll, H.; Stone, A. J.; Tarroni, R.; Thorsteinsson, T. *MOLPRO*, version 2000.6; University of Birmingham: Birmingham, U.K., 1999.
- Scott, A. P.; Radom, L. *J. Phys. Chem.* **1996**, *100*, 16502–16513.
- (a) Coote, M. L.; Wood, G. P. F.; Radom, L. *J. Phys. Chem. A* **2002**, *106*, 12124–12138. (b) Coote, M. L. *J. Phys. Chem. A* **2004**, *108*, 3865–3872. (c) Gómez-Balderas, R.; Coote, M. L.; Henry, D. J.; Radom, L. *J. Phys. Chem. A* **2004**, *108*, 2874–2883.
- Henry, D. J.; Sullivan, M. B.; Radom, L. *J. Chem. Phys.* **2003**, *118*, 4849–4860.
- See, for example: (a) Ah Toy, A.; Chaffey-Millar, H.; Davis, T. P.; Stenzel, M. H.; Izgorodina, E. I.; Coote, M. L.; Barner-Kowollik, C. *Chem. Commun.* **2006**, 835–837. (b) Coote, M. L.; Izgorodina, E. I.; Krensk, E. H.; Busch, M.; Barner-Kowollik, C. *Macromol. Rapid Commun.* **2006**, *27*, 1015–1022. (c) Izgorodina, E. I.; Coote, M. L. *Chem. Phys.* **2006**, *324*, 96–110.
- Izgorodina, E. I.; Brittain, D. R. B.; Hodgson, J. L.; Krensk, E. H.; Lin, C. Y.; Namazian, M.; Coote, M. L. *J. Phys. Chem. A* **2007**, *111*, 10754–10768.
- These formulas are described in full in: Coote, M. L. In *Encyclopedia of Polymer Science and Technology*, 3rd ed.; Kroschwitz, J. I. Ed.; Wiley: New York, 2004; Vol. 9, pp 319–371.
- See, for example: Ellingson, B. A.; Lynch, V. A.; Mielke, S. L.; Truhlar, D. G. *J. Chem. Phys.* **2006**, *125*, 084305.
- Lin, C. Y.; Izgorodina, E. I.; Coote, M. L. *J. Phys. Chem. A* **2008**, *112*, 1956–1964.
- Van Cauter, K.; Van Speybroeck, V.; Vansteenkiste, P.; Reyniers, M.-F.; Waroquier, M. *ChemPhysChem* **2006**, *7*, 131–140.
- Griller, D.; Ingold, K. *Acc. Chem. Res.* **1976**, *9*, 13–19.
- Handford-Styring, S. M.; Walker, R. W. *J. Chem. Soc., Faraday Trans.* **1995**, *91*, 1431–1438.
- Beckwith, A. L. J.; Schiesser, C. H. *Tetrahedron* **1985**, *41*, 3925–3941.
- See, for example: (a) Zammit, M. D.; Coote, M. L.; Davis, T. P.; Willett, G. D. *Macromolecules* **1998**, *31*, 955–963. (b) Fischer, H.; Radom, L. *Angew. Chem., Int. Ed.* **2001**, *40*, 1340–1371.
- (a) Beckwith, A. L. J.; Duggan, S. A. M. *J. Chem. Soc., Perkin Trans. 2* **1994**, 1509–1518. (b) Franz, J. A.; Roberts, D. H.; Ferris, K. F. *J. Org. Chem.* **1987**, *52*, 2256–2262.

JP806535Z